Phase-Change Heat Transfer in Microsystems

Ping Cheng[1]
e-mail: mepcheng@yahoo.com

Hui-Ying Wu

Fang-Jun Hong

School of Mechanical and Power Engineering,
Shanghai Jiaotong University,
800 Dong Chuan Road,
Shanghai 200240, P.R. China

Recent work on miscroscale phase-change heat transfer, including flow boiling and flow condensation in microchannnels (with applications to microchannel heat sinks and microheat exchangers) as well as bubble growth and collapse on microheaters under pulse heating (with applications to micropumps and thermal inkjet printerheads), is reviewed. It has been found that isolated bubbles, confined elongated bubbles, annular flow, and mist flow can exist in microchannels during flow boiling. Stable and unstable flow boiling modes may occur in microchannels, depending on the heat to mass flux ratio and inlet subcooling of the liquid. Heat transfer and pressure drop data in flow boiling in microchannels are shown to deviate greatly from correlations for flow boiling in macrochannels. For flow condensation in microchannels, mist flow, annular flow, injection flow, plug-slug flow, and bubbly flows can exist in the microchannels, depending on mass flux and quality. Effects of the dimensionless condensation heat flux and the Reynolds number of saturated steam on transition from annular two-phase flow to slug/plug flow during condensation in microchannels are discussed. Heat transfer and pressured drop data in condensation flow in microchannels, at low mass flux are shown to be higher and lower than those predicted by correlations for condensation flow in macrochannels, respectively. Effects of pulse heating width and heater size on microbubble growth and collapse and its nucleation temperature on a microheater under pulse heating are summarized. [DOI: 10.1115/1.2410008]

Keywords: boiling, condensation, phase change, bubble, nucleation

Introduction

Advances in microelectronic fabrication technology have led to the miniaturization of silicon components. This coupled with the improved processing speed in clock frequencies from MHz to GHz has generated increasingly larger amount of heat in microprocessors. The large amount of heat, if not properly dissipated, will cause overheating of a chip, leading to its degrading performance and eventual damage. To cope with the demand for more efficient cooling technology for the next generation of high power electronics devices, various kinds of microheat exchangers and two-phase microchannel heat sinks [1,2] have been developed in recent years. For this reason, a great deal of recent work has been devoted to the study of boiling and condensation in microchannels [3–23].

Meanwhile, advances in microfabrication also led to many Micro-Electrical-Mechanical-Systems (MEMS) products such as thermal inkjet printheads [24] and microthermal bubble pumps [25]. For thermal inkjet applications, microheaters under electrical pulse of several microseconds (μs) are used to generate a microbubble periodically. The microbubble will expel a small drop of ink through a nozzle at a high frequency to a specified position on a paper to compose the text and graphics. The quality of the print depends on the size of the drops and drop velocity, which are closely related to bubble nucleation. Recently, Deng et al. [26] found that if the pulse width applied to a microheater is increased from the microseconds to milliseconds level, the periods of bubble expansion and collapse are asymmetric. This characteristics can be used to design a thermal actuator or perturbator [26,27] and for DNA hybridization enhancement [28,29].

In this paper, we will review the most recent literature on flow boiling [3–18] and condensation [19–23] in microchannels with applications to microheat exchangers and microheat sinks, as well as bubble nucleation under pulse heating [25–31] with applications to microthermo-bubble actuators.

Classification of Microchannels

It is well known that the Bond number is an important parameter in phase change heat transfer [2,3]. The Bond number is defined as

$$\mathrm{Bo}_d = (D_h/\ell_c)^2 = g(\rho_\ell - \rho_v)D_h^2/\sigma \tag{1}$$

where $\ell_c=[\sigma/(\rho_\ell-\rho_v)g]^{1/2}$ is the capillary length; D_h is the hydraulic diameter of the channel; g is the gravitational acceleration; σ is the surface tension; and ρ_ℓ and ρ_v are density of the liquid and the vapor, respectively. Equation (1) shows that the Bond number is a ratio of the hydraulic diameter to the capillary length, which is also a measure of the relative importance of the buoyancy force to surface tension force. The classification of microchannels, minichannels, or macrochannel can be based on the Bond number as follows [2]:

1. Microchannel: if $\mathrm{Bo}_d<0.05$ where gravity effect can be neglected;
2. Minichannel: if $0.05<\mathrm{Bo}_d<3.0$ where surface tension effect becomes dominant and gravitational effect is small; and
3. Macrochannel: if $\mathrm{Bo}_d>3.0$ where surface tension is small in comparison with gravitational force.

It is relevant to point out that the Bond number, defined by Eq. (1), has taken into consideration the effects of temperature, pressure, and physical properties of the fluid. According to the above classification, a channel with its hydraulic diameter less than 490 μm (at 450 K) or 600 μm (at 300 K), respectively, is considered to be a microchannel for phase change heat transfer if water is used as the working medium.

[1]Corresponding author.

Contributed by the Heat Transfer Division of ASME for publication in the JOURNAL OF HEAT TRANSFER. Manuscript received August 4, 2006; final manuscript received September 20, 2006. Review conducted by Yogesh Jaluria. Paper presented at the International Heat Transfer Conference 2006. Max Jakob Award Lecture.

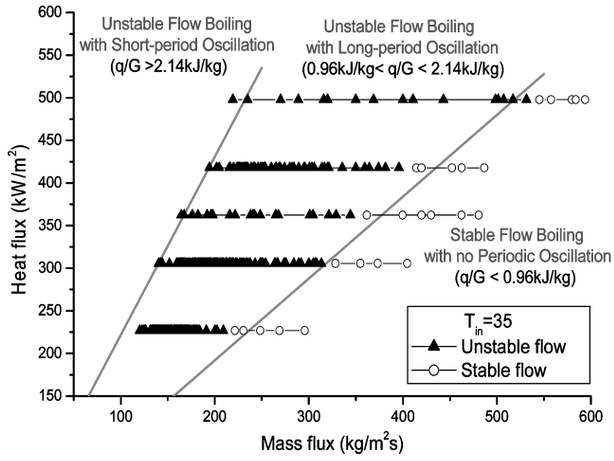

Fig. 1 Flow boiling regimes in microchanels [14]

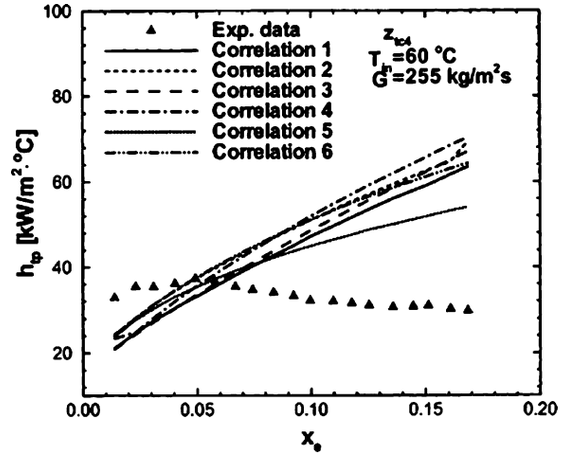

Fig. 2 Comparison of measurements of local heat transfer coefficient in flow boiling of water in microchannel with correlation equations for macrochannels [7]

Flow Boiling in Microchannel

Flow Patterns. Hetsroni et al. [4] investigated flow boiling of water in silicon microchannels having hydraulic diameters of 103 μm and 129 μm, respectively, and observed periodic annular flow and periodic dry steam flow in the microchannels. In another paper, Hetsroni et al. [5] performed a flow boiling experiment on Vertrel XF fluid in silicon microchannels of triangular cross section, having a hydraulic diameter of 130.14 μm. They measured low-amplitude/short-period fluctuations in the pressure drop and outlet fluid temperature, which were attributed to the growth and collapse of vapor bubbles in the two-phase flow. Qu and Mudawar [6] performed a flow boiling experiment of water in a two-phase microchannel heat sink, and identified two types of instability in microchannels: severe pressure drop oscillation and mild parallel channel instability. They discussed the possibility of reverse vapor flow. Lee et al. [7] and Li et al. [8] found that reverse flow exists in both single and multiple microchannels. Most recently, Hetsroni et al. [9] performed an experiment on flow boiling of water in a microchannel with a hydraulic diameter of 250 μm for mass flux in the range of 95–340 kg/m^2 s and heat flux in the range of 80–330 kW/m^2. They observed explosive boiling with periodic wetting and dryout in the microchannels.

Wu et al. [10–12] carried out a series of experiments on the simultaneous visualization and measurements on flow boiling in parallel silicon microchannels having a hydraulic diameter ranging from 49.9 μm to 186 μm. It was found that large temperature and pressure fluctuations with long oscillation periods occurred under certain heat and mass flux conditions. Most recently, a more systematical investigation on flow boiling patterns has been carried out by Wang et al. [13], who show that stable and unstable flow patterns occur in microchannels, depending on the values of heat to mass flux ratio q/G and inlet subcooling. Note that the boiling number Bo_i is related to q/G by

$$\mathrm{Bo}_i = \frac{q}{Gh_{fg}} \tag{2}$$

Figure 1 shows that the following three flow boiling modes exist in microchannels having a hydraulic diameter of 186 μm at an inlet subcooling of 35°C:

1. Stable flow boiling mode for $q/G < 0.96$ J/g: This is a stable flow boiling regime with no temporal temperature and pressure variations. Isolated bubbles are generated near the inlet and are carried away downstream by the bulk flow.

2. Unstable flow boiling mode with long-period oscillation for $0.96 \text{ J/g} < q/G < 2.14$ J/g: elongated bubbles expand upstream because of the limited transverse space in the microchannels. Elongated bubbles expand upstream to near the inlet of the microchannels, which becomes an annular/mist flow. The incoming cooled liquid pushes the elongated bubbles back to downstream, and isolated bubbles being generated upstream are carried away to downstream by the cooler incoming liquid. Thus, isolated bubbles flow and annular/mist flow appear alternatively with time in the microchannels. This leads to cyclic variations of wall temperatures and inlet pressure. As a result, the inlet wall temperature is gradually increased until it reaches an equilibrium state, where small temporal temperature variation was observed.

3. Unstable flow boiling mode with short-period oscillation for $q/G > 2.14$ J/g: This is an unstable flow boiling regime with the inlet wall temperature near saturated condition, and small temporal temperature variation is observed. Annular flow and mist flow may appear alternatively with time in the microchannels. Small cyclic variations of inlet pressure with short periods occur in the microchannels.

Heat Transfer Characteristics. Qu and Mudawar [6] performed an experiment on flow boiling of water in microchannels with a hydraulic diameter of 0.349 mm. Figure 2 shows that the measured local heat transfer coefficient decreased with the vapor quality, and it was pointed out that this behavior was contradictory to existing correlations for macrochannels. Yen et al. [14] obtained the local heat transfer coefficient for flow boiling of water at a flow rate G of 295 kg/m^2 s and a heat flux q in the range of 1–13 kW/m^2 s in microchannels having a hydraulic diameter of 0.51 mm. They found that the local heat transfer coefficient is independent of mass flux, but is a strong function of heat flux. They also found that the local heat transfer coefficient decreases with vapor quality. The local boiling heat transfer coefficient decreasing with vapor quality was also confirmed by Hetsroni et al. [9], who performed an experiment on flow boiling of water in microchannels with triangular cross sections having a hydraulic diameter of 144 μm at $G = 95–340$ kg/m^2 s and $q = 80–330$ kw/m^2. Sumith et al. [15] obtained heat transfer coefficient for flow boiling of water in minichannels with a hydraulic diameter of 1.45 mm at $G = 23.4–152.7$ kg/m^2 s, and $q = 10–715$ kW/m^2. As shown in Fig. 3, their measured heat transfer coefficients for $q > 200$ kW/m^2 were in agreement with correlation equations for macrochannels. However, their measurements for $q < 200$ kW/m^2 were higher than those predicted by correlation equations for macrochannels.

Most recently, Lee and Mudawar [16] carried out an experimental investigation for flow boiling of R-134a in microchannels having a hydraulic diameter of 0.349 mm. They found that boiling

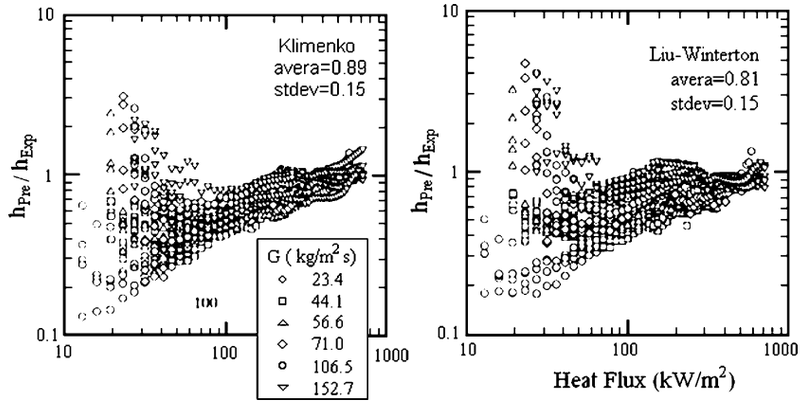

Fig. 3 Comparison of boiling heat transfer coefficient in minichannels with existing correlations for macrochannels [16]

heat transfer coefficient of R-134a in microchannels cannot be predicted by existing correlation equations for flow boiling in macrochannels. Since boiling heat transfer mechanisms are different for low, medium, and high vapor qualities, they proposed different correlations for these three quality regimes. As in correlations for flow boiling in macrochannels, the Martinelli number is an important parameter in these three quality regimes in microchannels. However, whereas the Martinelli parameter is raised to a positive exponent in microchannel correlations, it was raised to a negative exponent in macrochannel correlation equations. In addition to the Martinelli parameter, they showed that the boiling number and the Weber number are also important parameters in the correlation of flow boiling heat transfer in the medium vapor qualities regime. It was found that their proposed correlations are in good agreement with their flow boiling heat transfer coefficient data in microchannels.

Pressure Drop Characteristics. Lee and Mudawar [17] carried out an experiment for pressure drop in flow boiling of R-134a in a microchannel with a hydraulic diameter of 0.349 mm at $G=127-654$ kg/m^2 s and $q=31.6-93.8$W/cm^2. A comparison of their experimental data with existing correlation equations for pressure drop in macrochannels is presented in Fig. 4. It is shown that the pressure drop data in microchannels deviated greatly from those predicted by macrochannel correlations. Taking the surface tension effect into consideration, they proposed a modified Lockhart–Martinelli correlation with the additional parameters of Weber number and Reynolds number, which can predict their pressure drop data well.

Tran et al. [18] obtained pressure drop data in flow boiling of three refrigerants (R-134a, R-12, and R-113) in minichannels with hydraulic diameters of 2.46 and 2.92 mm, respectively. They compared their experimental data for minichannels with several existing correlations for macrochannels, and found that most of these existing correlations underpredicted the pressure drop in minichannels as shown in Fig. 5. They speculated that greater pressure drop in a microchannel may be due to additional friction relating to the movement of elongated bubbles. They proposed a modified B coefficient correlation taking into consideration the confinement of bubbles in microchannels. Their modified correlation for pressure drop in flow boiling of the three refrigerants agrees within ±20% of their measurements.

Condensation in Microchannels

Flow Patterns. Chen and Cheng [19] performed a flow visualization study on condensation of saturated steam in a silicon micorchannel with a hydraulic diameter of 75 μm. They found that mist flow with microwater droplets existed near the inlet of the microchannels and intermittent flow near the outlet. Subsequently, Wu and Cheng [20] carried out simultaneous visualization and measurement experiments on saturated steam condensing in parallel silicon microchannels with a length of 30 mm, having a trapezoidal cross section with a hydraulic diameter of 82.6 μm. They observed that mist flow, annular flow, slug/bubbly flow, and bubbly flow existed from upstream to downstream in the microchannels, as shown in Fig. 6. The transition from annular to slug/bubbly flow, which was clearly shown for the first time, is called the injection flow.

Most recently, Quan et al. [21] carried out a visualization study to investigate the effects of dimensionless condensation heat flux and Reynolds number of the saturated steam on the transition from annular flow to slug/bubbly flow in condensation in microchannels. The results are presented in Fig. 7 where Z/L is the dimensionless location of the transition (with L denoting the

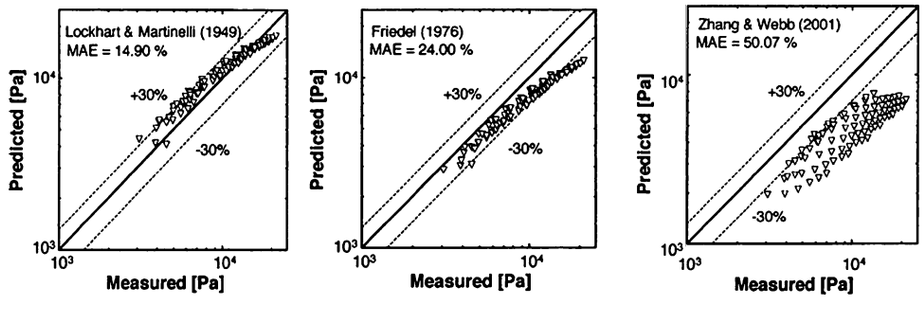

Fig. 4 Comparison of pressure drop data for flow boiling of R134a in microchannels with existing correlations for flow boiling in macrochannels [18]

length of the microchannels); Re is the Reynolds number of the steam; and $\tilde{q}=q_c/Gh_{fg}$ is the dimensionless condensation heat flux with q_c denoting the condensation heat flux. It is shown that the value of Z/L decreases (implying that injection flow occurs further upstream) with increasing $\tilde{q}$ or decreasing Re.

Heat Transfer Characteristics. Shin and Kim [22] carried out an experiment on condensation of R134a in a microchanel with a hydraulic diameter of 0.493 mm. Figure 8 shows that their measured Nusselt numbers in the microchannels were higher than those predicted by the existing correlations for macrochannels at low mass fluxes ($G<200$ kg/m^2 s). On the other hand, their measured Nusselt numbers at high mass flux ($G>200$ kg/m^2 s) can be reasonably well predicted by existing correlations for macrochannels.

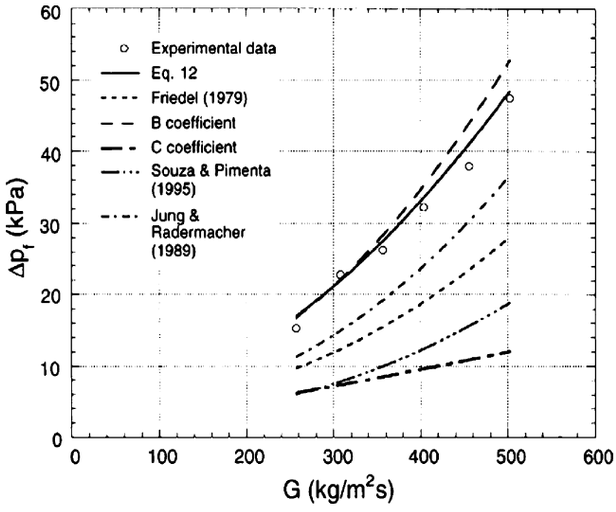

Fig. 5 Correlation of pressure drop of refrigerants in flow boiling in minichannels [19]

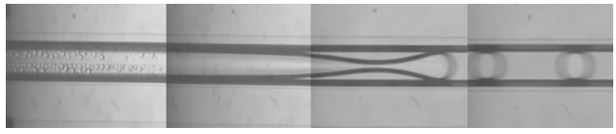

Fig. 6 Photos of condensation flow in microchannels with D_h=82.6 μm at m=30.4 g/cm^2 s [20]

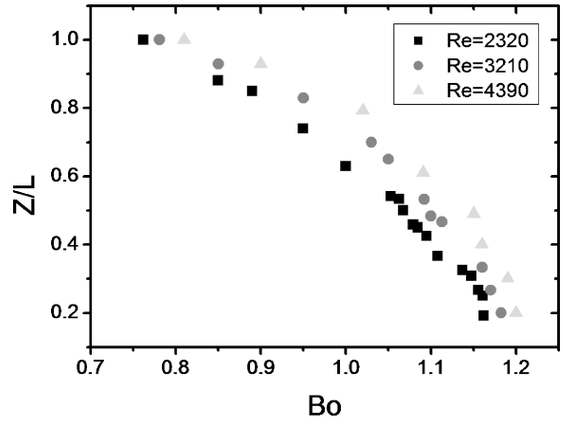

Fig. 7 Transition from annular to slug/bubbly flow in condensation of steam in microchannels [21]

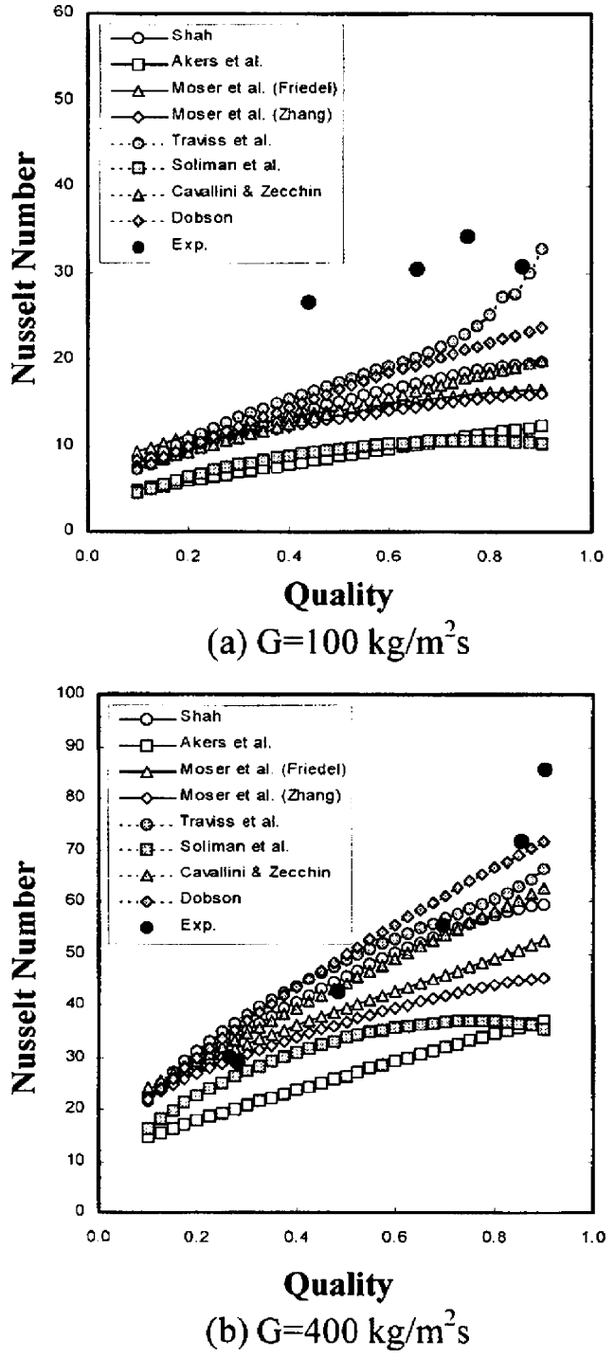

Fig. 8 Comparison of measured Nusselt number for condensation of R134a in microchannels with macrochannel correlation equation [23]

Pressure Drop Characteristics. Kim et al. [23] obtained pressure drop measurements for condensation flow of R134a in a microchannel having a hydraulic diameter of 0.691 mm. Figure 9 shows a comparison of their measurements with existing correlation equations for macrochannels. It is shown that at low mass flux ($G<200$ kg/m^2 s), the pressure drop in condensation flow in a microchannel is lower than that predicted by Friedel's correlation for macrotubes. At higher mass fluxes ($G>200$ kg/m^2 s), however, pressure drop in condensation flow in a microchannel can be predicted well by Friedel's correlation for macrotubes.

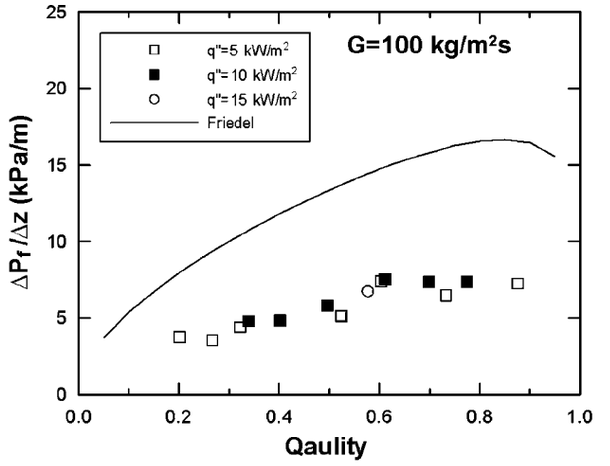

Fig. 9 Comparison of measured pressure drop versus quality for condensation flow of R-134a in a microchannel having D =0.691 mm with Friedel's correlation equation for macrochannels [23]

Bubble Nucleation Under Pulse Heating

As mentioned in the Introduction, microbubble nucleation under pulse heating has important applications to thermal inkjet printheads, vapor bubble pumps, and vapor bubble perturbators. Single bubbles can be generated periodically in these devices on a microheater under pulse heating with different pulse widths. For thermal inkjet printheads, bubbles are generated in the microsecond (μs) range. On the other hand, bubbles are generated in the millisecond (ms) range in vapor-bubble pumps and in vapor-bubble perturbators. Under rapid pulse heating, power densities equivalent to several megawatts per square meter can be generated. Bubble nucleation under an extremely high heat flux pulse differs from the usual nucleate boiling in many aspects. First, bubble nucleation is initiated at a higher temperature close to the theoretical superheat limit. Second, the boiling process is more explosive because the initial bubble pressure is very high. Third, the boiling process is more reproducible because its mechanism is governed by the property of the liquid (i.e., homogeneous nucleation) rather than by the surface characteristics (i.e., heterogeneous nucleation).

Effects of Pulse Width on Bubble Growth and Collapse. Deng et al. [26] performed an experiment to investigate the bubble growth and collapse on a nonuniform width microheater under pulse heating width in the millisecond range for the purpose

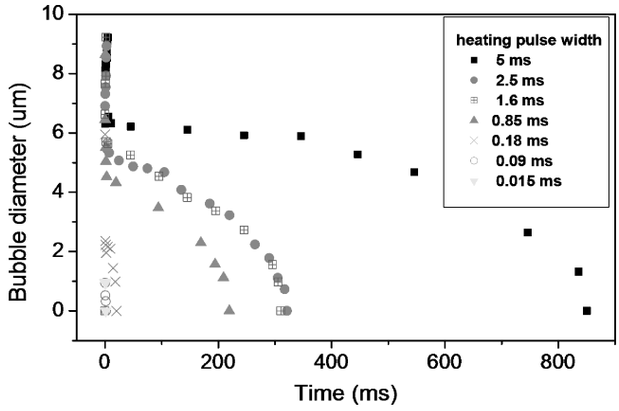

Fig. 10 Effects of pulse width on bubble growth and collapse on a 3×10 μm² microheater submerged in DI water [27]

of enhancing DNA hybridization [28–30]. Figure 10 shows the effect of pulse width τ on bubble growth and collapse on a nonuniform microheater with the slim part having a size of 10 $\times 3$ μm^2. It is shown that there is a rapid bubble expansion period followed by a slow bubble collapse period. The asymmetric bubble expansion and collapse periods lead to perturbation of the fluid. Moreover, a longer pulse width leads to a longer lifetime of a bubble. The case of τ=1.66 ms was chosen for further study because this pulse width can lead to reasonable perturbation of fluid without introducing a large amount of heat.

Effects of Heater Size on Nucleation and Bubble Shape. Recently, Deng et al. [31] have performed an experiment to study effects of the heater size on bubble shape and onset of nucleation under a 1.66 ms pulse heating. Table 1 listed the dimensions of the submicron and micron heaters used in their experiments. Figure 11 shows the effect of heater size on nucleation temperature and nucleation time at a pulse width of 1.66 ms. It is shown that the nucleation temperature decreases while the nucleation time increases as the heater size is increased. This is because the temperature rise rate of the heater decreases with the heater size. It was also found that there existed a critical feature size of the heater, 10 μm, for this pulse width. The bubble shape for heaters with feature size below or above this critical value was quite different. Thus, the bubble generated by heaters can be classified into two groups as shown in Fig. 12. Single spherical bubble was generated periodically with Group I heaters (a)–(f) with the width of the slim part of the heater less than or equal to 10 μm, and an oblate vapor blanket was generated periodically with Group II heaters (g)–(k). The fact that the shape of the bubble and boiling

Table 1 Dimensions of various submicron and micron heaters used in Deng et al.'s experiments [31]. The length and width are those of the slim part of the heater.

Heater ID	Length ±2% (μm)	Width ±3% (μm)
(a)	0.5	0.5
(b)	1	0.5
(c)	2	1
(d)	10	3
(e)	10	5
(f)	20	10
(g)	30	10
(h)	30	15
(i)	90	30
(j)	150	50
(k)	200	70

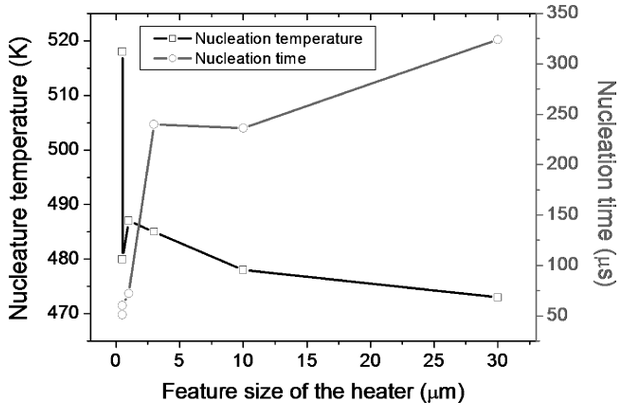

Fig. 11 Effects of heater size on nucleation temperature and nucleation time at pulse width of 1.66 ms [31]

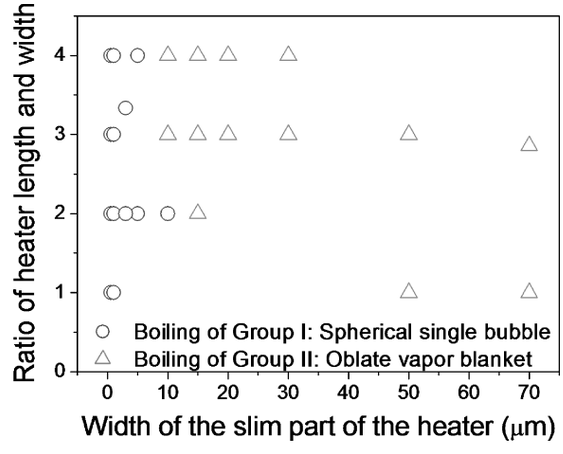

Fig. 12 Effect of heater size on bubble shapes at pulse width of 1.66 ms [31]

pattern depends on the slim part of the heater can be explained as follows: after the occurrence of incipience of boiling, the water–vapor interface will try to form a spherical shape within the thin superheated liquid due to the surface tension effect, which is the dominant force at the microscale level. The spherical bubble begins to shrink when it grows near the outer edge of the thin superheated region because of the condensation effect. When the heater has exceeded a certain critical length, the spherical bubble cannot fit in the thin superheated region, and it grows to fit the thin superheated region as an elongated bubble on the heater. Because of the larger exposed area of the elongated bubble to outer cooled fluid, the condensation effect is much stronger than the spherical bubble. It then collapses immediately thereafter.

Concluding Remarks

Recent work on phase-change heat transfer processes in microsystems has been reviewed in this paper. The following conclusions can be drawn.

For Flow Boiling in Microchannels.

1. Bubbly flow (isolated bubble), plug/slug flow (confined bubble), annular flow, and mist flow may exist in flow boiling in microchannels.
2. In the stable flow boiling mode (see Fig. 1), vapor bubbles grow on the heated wall, elongated, and are carried away by the liquid to downstream. No temporal pressure and temperature variations have been observed in the microchannels under these conditions.
3. In the unstable flow boiling mode with long-period oscillation (Fig. 1), cyclic variations of temperature and pressure have been observed. During one cycle, bubbly flow changes to annular/mist flow and then changes to bubbly flow again. The annular flow is formed when confined vapor bubbles expand in both upstream and downstream directions, resulting in the increase of wall temperature and inlet water temperature. As a result, both wall temperature and inlet water temperature increase gradually with time, and amplitudes of oscillation decrease with time while the oscillation period increases with time. The oscillation flow becomes stable after an equilibrium condition is reached.
4. In the unstable flow boiling mode with short-period oscillation (Fig. 1), annular flow and mist flow appear, alternating in time in the microchannels. Periodic dryout and rewetting have been observed under these conditions. This is an unstable flow boiling mode where temperature and inlet pressure oscillations are small.
5. Both boiling heat transfer coefficient and pressure drop data in microchannels cannot be predicted by existing correlations obtained for macrochannels.

For Condensation Flow in Microchannels

1. There are four flow patterns in flow condensation in microchannels: mist flow, annular flow, slug/plug flow (confined bubble), and bubbly flow (isolated bubble).
2. The transition from annular flow to slug/plug flow during flow condensation takes place further downstream in the microchannels as the dimensionless heat transfer rate is increased, or as the Reynolds number is decreased.
3. At low mass fluxes ($G<200$ kg/m^2 s), measured Nusselt numbers for condensation in microchannels are higher than predicted from correlations for macrochannels. At high mass fluxes ($G>200$ kg/m^2 s), the measured Nusselt numbers in microchannels can be predicted well with existing correlations for macrochannels.
4. At low mass fluxes ($G<200$ kg/m^2 s), measured pressure drop data for condensation flow in microchannels is lower those predicted by Friedel's correlation for macrotubes. At high mass fluxes ($G>200$ kg/m^2 s), the measured pressure drop data can be predicted well with existing correlations for macrochannels.

For Microbubble Generation Under Pulse Heating

1. A single microbubble can be generated periodically by a nonuniform width microheater under pulse heating.
2. When the pulse width of a microheater is in the microsecond range, the growth and collapse periods of a microbubble are symmetric.
3. When the pulse width of a microheater is in the millisecond range, a rapid expansion period and a slow collapse period are observed. The rapid expansion period is pressure control while the slow collapse period is thermal control. The asymmetric expansion and collapse periods lead to flow perturbations.
4. Whether it is a spherical vapor bubble or oblate vapor blanket on the heater depends on the pulse width and heater size.

Acknowledgment

This work was supported by the National Natural Science Foundation of China through Grant Nos. 50536010 and 50476017, and by Shanghai Municipal Science and Technology Committee through Grant No. 05JC14025.

Nomenclature

Bo_d = Bond number

Bo_i = boiling number
D_h = hydraulic diameter (m)
g = gravity ($\mathrm{m/s^2}$)
G = mass flux ($\mathrm{kg/m^2\,s}$)
h = enthalpy (J/kg)
h_{fg} = latent of heat of evaporation (J/kg)
L = length of the microchannel (m)
ℓ_{c} = capillary length (m)
q = heat flux ($\mathrm{kW/m^2}$)
x = vapor quality
Z = distance from the inlet (m)

Greek Symbols

μ = dynamic viscosity ($\mathrm{N\,s/m^2}$)
ρ = density ($\mathrm{kg/m^3}$)
σ = surface tension (N/m)

References

[1] McGlen, R. J., Jachuck, R., and Lin, S., 2004, "Integrated Thermal Management Techniques for High Power Electronic Devices," Appl. Therm. Eng., **24**, pp 1143–116.
[2] Cheng, P., and Wu, H. Y., 2006, "Mesoscale and Microscale Phase-Change Heat Transfer," Adv. Heat Transfer, **39**, pp. 461–563.
[3] Kandlikar, S. G., 2004, "Heat Transfer Mechanism During Flow Boiling in Microchannels," J. Heat Transfer, **126**, pp. 8–16.
[4] Hetsronic, G., Mosyak, A., and Segal, Z., 2001, "Nonuniform Temperature Distribution in Electronic Devices Cooled by Flow in Parallel Microchannels," IEEE Trans. Compon. Packag. Technol., **24**, pp. 7–23.
[5] Hetsronic, G., Mosyak, A., Segal, Z., and Ziskind, G. A., 2002, "A Uniform Temperature Heat Sink for Cooling of Electronic Devices," Int. J. Heat Mass Transfer, **45**, pp. 3275–3286.
[6] Qu, W., and Mudawar, I., 2003, "Flow Boiling Heat Transfer in Two-Phase Microchannel Heat Sinks-I. Experimental Investigation and Assessment of Correlation Methods," Int. J. Heat Mass Transfer, **46**, pp. 2755–2771.
[7] Lee, P. C., Tseng, F. G., and Pan, C., 2004, "Bubble Dynamics in Microchannels. Part I: Single Microchannel," Int. J. Heat Mass Transfer, **47**, pp. 5575–5589.
[8] Li, H. Y., Tseng, F. G., and Pan, C., 2004, "Bubble Dynamics in Microchannels. Part II: Two Parallel Microchannels," Int. J. Heat Mass Transfer, **47**, pp. 5591–5601.
[9] Hetsroni, G., Mosyak, A., Pogrebnyak, E., and Segal, Z., 2005, "Explosive Boiling of Water in Parallel Microchannels," Int. J. Multiphase Flow, **31**, pp. 371–392.
[10] Wu, H. Y., and Cheng, P., 2003, "Visualization and Measurements of Periodic Boiling in Silicon Microchannels," Int. J. Heat Mass Transfer, **46**, pp. 2603–2614.
[11] Wu, H. Y., and Cheng, P., 2003, "Liquid/Two-Phase/Vapor Alternating Flow During Boiling in Microchannels at High Heat Flux," Int. Commun. Heat Mass Transfer, **30**, pp. 295–302.
[12] Wu, H. Y., and Cheng, P., 2004, "Boiling Instability in Parallel Silicon Microchannels at Different Heat Flux," Int. J. Heat Mass Transfer, **47**, pp. 3631–3641.
[13] Wang, G. D., Cheng, P., and Wu, H. Y., 2006, "Stable and Unstable Flow Boiling in Microchannels," Int. J. Heat Mass Transfer (in press).
[14] Yen, T. H., Kasagi, N., and Suzuki, Y., 2003, "Forced Convective Boiling Heat Transfer in Microtubes at Low Mass and Heat Fluxes," Int. J. Multiphase Flow, **29**, pp. 1771–1792.
[15] Sumith, B., Kaminaga, F., and Matsumura, K., 2003, "Saurated Flow Boiling of Water in a Vertical Small Diameter Tube," Exp. Therm. Fluid Sci., **27**, pp. 789–801.
[16] Lee, J., and Mudawa, I., 2005, "Two-Phase Flow in High Heat Flux Microchannel Heat Sink for Refrigeration Cooling Applications: Part II-Heat Transfer Characteristics," Int. J. Heat Mass Transfer, **48**, pp. 941–955.
[17] Lee, J., and Mudawa, I., 2005, "Two-Phase Flow in High-Heat Flux Microchannel Heat Sink for Refrigeration Cooling Applications: Part I-Pressure Drop Characteristics," Int. J. Heat Mass Transfer, **48**, pp. 928–940.
[18] Tran, T. N., Chyu, M. C., Wambsganss, M. W., and France, D. M., 2000, "Two-Phase Pressure Drop of Refrigerants During Flow Boiling in Small Channels: An Experimental Investigation and Correlation Development," Int. J. Multiphase Flow, **26**, pp. 1739–1754.
[19] Chen, Y. P., and Cheng, P., 2005, "Condensation of Steam in a Silicon Microchannel," Int. Commun. Heat Mass Transfer, **32**, pp. 175–183.
[20] Wu, H. Y., and Cheng, P., 2005, "Condensation Flow Patterns in Silicon Microchannels," Int. J. Heat Mass Transfer, **48**, pp. 2186–2197.
[21] Quan, X. J., Cheng, P., and Wu, H. Y., 2006, Transition from Annular to Slug/Bubbly Flow in Condensation in Microchannels, unpublished.
[22] Shin, J. S., and Kim, M. H., 2004, "An Experimental Study of Flow Condensation Heat Transfer Inside Circular and Rectangular Minichannels," *Proc. of* $2\mathrm{P}^{\mathrm{ndP}}$ *International Conference, on Microchannel and Microchannels*, pp. 633–640.
[23] Kim, M. H., Shin, J. S., Huh, C., Ki, T. J., and Seo, K. W., 2003, "A Study of Condensation Heat Transfer in a Single Mini-tube and a Review of Korean Micro-and Mini-Channel Studies," *Proceedings of the 1st International Conference on Microchannel and Minichannels, Rochester, NY, 24–25 April 2003*, pp. 47–58.
[24] Kobayashi, H., Koumura, N., and Ohno, S., 1981, "Canon Kabushiki Kaisha Liquid Recording Medium," US Patent Specification No. 4243994.
[25] Yin, Z., Prosperetti, A., and Kim, J., 2004, "Bubble Growth on an Impulsively Powered Microheater," Int. J. Heat Mass Transfer, **47**, pp. 1053–1067.
[26] Deng, P. G., Lee, Y. K., and Cheng, P., 2003, "The Growth and Collapse of a Micro-bubble under Pulse Heating," Int. J. Heat Mass Transfer, **46**, pp. 4041–4050.
[27] Okamoto, T., Suzuki, T., and Yamamoto, N., 2000, "Microarray Fabrication With Covalent Attachment of DNA using Bubble Jet Technology," Nat. Biotechnol., **18**, pp. 438–441.
[28] Deng, P. G., Lee, Y. K., and Cheng, P., 2006, "Two-Dimensional Micro-Bubble Actuator Array to Enhance Efficiency of Molecular Beacon Based DNA Micro-Biosensors," Biosens. Bioelectron., **21**, pp. 1443–1450.
[29] Deng, P. G., Lee, Y. K., and Cheng, P., 2004, "Micro Bubble Dynamics in DNA Solutions," J. Micromech. Microeng., **14**, pp. 693–701.
[30] Deng, P. G., Lee, Y. K., and Cheng, P., 2005, "Measurements of Micro Bubble Nucleation Temperatures in DNA Solutions," J. Micromech. Microeng., **15**, pp. 564–574.
[31] Deng, P. G., Lee, Y. K., and Cheng, P., 2006, "An Experimental Study of Heater Size Effects on Microbubble Generation," Int. J. Heat Mass Transfer, **49**, pp. 2535–2544.